American Mineralogist, Volume 81, pages 213–225, 1996

The origin and diagenesis of grain-coating serpentine-chlorite in Tuscaloosa Formation sandstone, U.S. Gulf Coast

P.C. Ryan* and R.C. Reynolds Jr.

Department of Earth Sciences, Dartmouth College, Hanover, New Hampshire 03755, U.S.A.

Abstract

Randomly interstratified serpentine-chlorite (Sp-Ch) is ubiquitous in sandstones of the subsurface Tuscaloosa Formation. The Sp-Ch occurs as grain coatings, pore fillings, peloids, and infillings. The presence of peloids and infillings suggests that the Sp-Ch originated as odinite, a 7 Å mineral that forms at the sediment-seawater interface in shallow, tropical marine sediments. We conclude that during the very earliest stages of diagenesis, odinite peloids and infillings transformed to mixed-layer Sp-Ch, forming grain coatings with preservation of some of the original odinite textures. The formation of grain-coating Sp-Ch during early diagenesis apparently preserved high primary porosity in medium-grained specimens. Fine-grained and silty sandstones, however, contain poorly formed grain coatings and are tightly cemented by quartz, implying that grain size also has some effect on authigenic quartz growth.

With increasing burial depth between 1702 and 6216 m, the proportion of Sp layers in Sp-Ch decreases from 20.7 ± 1.1 to 1.3 ± 0.1%, indicating that Sp layers transform to Ch layers with increasing diagenetic grade. The polytype of the Sp-Ch is essentially I*bb* at depths <2000 m. At depths >2000 m, the polytype is randomly interstratified I*bb*-I*aa*, and the proportion of I*bb* layers decreases from ~100 to 49% over the interval studied. At depths <2000 m, orthohexagonal Sp transforms to I*bb* Ch, but at depths >2000 m, orthohexagonal Sp transforms to I*aa* Ch. There is essentially no change in Sp-Ch chemical composition with depth, implying that temperature is the dominant control on the structural transformations. Mean crystallite thickness also remains relatively constant with increasing depth, indicating that diagenetic transformations in Sp-Ch do not involve crystal-growth mechanisms typical of most clay minerals. Rather, the mineralogic transformations appear to proceed on a layer-by-layer basis, with individual layers dissolving and reprecipitating within the confines of the crystallites.

Introduction

Authigenic chlorite (Ch) is a common authigenic mineral in sandstone, often comprising the majority of the clay-size fraction. The occurrence of Ch as a coating on detrital grains is particularly interesting because the coating may inhibit quartz cementation, resulting in the preservation of abnormally high primary porosity in deeply buried rocks (e.g., Heald and Anderegg 1960; Pittman and Lumsden 1968; Thomsen 1982). Grain-coating Ch has been the subject of several recent studies (e.g., Thomsen 1982; Reynolds et al. 1992; Ehrenberg 1993; Hillier 1994; Spötl et al. 1994), but the origin of the Ch is uncertain, as are the effects of burial diagenesis on polytypism and mixed layering of Ch and interstratified 7 Å layers like those of serpentine (Sp) (e.g., Reynolds 1988; Walker 1993). Accordingly, the primary purposes of this study are (1) to determine the origin of diagenetic serpentine-chlorite (Sp-Ch) in Tuscaloosa Formation sandstone and (2) to examine the effects of burial diagenesis on mixed layering and polytypism of Sp-Ch in the Tuscaloosa Formation. (In this paper, the 7 Å layers that are interstratified with Ch are termed Sp, rather than the more specific mineral name berthierine, to avoid genetic implications associated with the name berthierine.)

In sandstone, authigenic Ch and related mixed-layer minerals commonly occur as grain coatings and pore fillings. They may form during the dissolution of kaolinite (Boles and Franks 1979; Burton et al. 1987) or volcanic rock fragments (Thomsen 1982), when Fe and Mg are liberated during illitization (Hower et al. 1976; Boles and Franks 1979), or by the transformation of a 7 Å phase to 14 Å Ch (Nelson and Roy 1958; Bailey 1988a; Hillier 1994). Two 7 Å clay minerals, berthierine and odinite, are structurally and chemically similar to Fe-rich Ch and occur in similar rocks. Odinite is a Sp-group, Fe-rich mineral that forms in tropical, shallow marine sediments at the seawater-sediment interface. It occurs as pellets and infillings and has site occupancy intermediate to those

* Present address: Environmental Sciences Department, Salish Kootenai College, Pablo, Montana 59855, U.S.A.

0003–004X/96/0102–0213$05.00

of trioctahedral and dioctahedral layers because of high amounts of Fe^{3+} (Odin 1985; Bailey 1988a). Berthierine is a trioctahedral Sp-group mineral that commonly occurs as ooids in unmetamorphosed iron formations and some shallow marine sandstones (Velde et al. 1974; Bhattacharyya 1983; Velde 1989), as well as in coal measures (Iijima and Matsumoto 1982) and altered igneous rocks (Ruotsala et al. 1964; Slack et al. 1992; Jiang et al. 1994).

Interstratification of Ch (14 Å) and Sp (7 Å) in sedimentary rocks has been documented by both X-ray diffraction (XRD) and transmission electron microscopy (TEM). Brindley and Gillery (1954) used XRD to document randomly interstratified kaolinite-chlorite, which was later interpreted as Sp-Ch by Brindley (1961). More recently, Dean (1983), Moore and Hughes (1990, 1991), and Reynolds et al. (1992) studied grain-coating Ch in sandstone, and they attributed broadening of Ch odd-order 00*l* peaks to randomly interstratified Sp layers. Walker and Thompson (1990) and Hillier (1994) also measured peak broadening and showed that the proportion of Sp layers in mixed-layer Sp-Ch decreases as temperature increases. Ahn and Peacor (1985) used TEM to document mixed-layer berthierine-chlorite in shales of the Gulf Coast Basin and indicated that the interlayered berthierine may be a metastable precursor to Ch under burial diagenetic conditions. These occurrences of mixed-layer Sp-Ch may represent intermediate stages in the prograde transformation of a 7 Å phase (e.g., odinite, berthierine) to Ch. The transformation requires the inversion of a tetrahedral sheet and may occur with no change in composition (Brindley 1961; Jiang et al. 1994). Nelson and Roy (1958) showed that synthesized 7 Å phases transform to Ch with increasing temperature, and Iijima and Matsumoto (1982) and Velde (1989) indicated that berthierine ooids transform to Ch during burial diagenesis of coal measures and ironstones. Bailey (1988a) found that 7 Å odinite transforms to Ch of the I*ba* polytype during early diagenesis of tropical marine sediments. These conclusions, when considered in conjunction with the findings of Walker and Thompson (1990) and Hillier (1994), suggest that the transformation of 7 Å phases to Ch could be used as an indicator of diagenesis and low-grade metamorphism in sandstone, ironstone, and coarse-grained limestone, rocks in which illite-smectite is often a minor or absent phase and thus is of no use in determining thermal history.

The naturally occurring Ch polytypes are I*aa,* I*ba* (I*b* $\beta = 97°$), I*bb* (I*b* $\beta = 90°$), and II*b* (Brown and Bailey 1962; Bailey 1988b; Walker 1993). Brown and Bailey (1962) first derived the structures of the Ch polytypes and showed that the II*b* polytype, which commonly occurs in greenschist facies rocks, has the most stable atomic configuration. The type-I polytypes have less stable atomic configurations and should transform to the II*b* polytype with increasing grade. Brown and Bailey (1962) also indicated that I*aa* Ch is stable at slightly higher temperatures than the I*bb* polytype, citing the prograde recrystallization of the I*bb* polytype to the I*aa* polytype in ironstone. Hayes (1970) studied Ch polytypes from a wide variety of rock types and geologic environments and proposed that the II*b* polytype is stable above 200 °C. The lower temperature polytypes, in order of increasing stability, are I*b* (disordered), I*ba,* and I*bb,* which, in theory, should sequentially transform to the stable II*b* polytype if sufficient energy is added to the system. However, few field studies have documented Ch-polytype transformations (Karpova 1969; Hillier 1994; Spötl et al. 1994), and II*b* is often the only Ch polytype in diagenetic and low-grade metamorphic sequences (Walker 1989; Walker and Thompson 1990; Ryan and Thompson 1991; Hillier 1993). Walker (1989) noted that type-I chlorites are rarely found in fine-grained rocks and suggested that the type-I polytypes require large pores or vugs in which to crystallize (e.g., sandstones, coarse-grained limestones, and veins). On the basis of studies of sedimentary and low-grade metamorphic rocks, it appears that Ch polytypism depends on more than temperature and is probably also controlled by factors such as P_{H_2O}, chemical composition, and time (Walker 1993). For a thorough discussion and review of Ch-polytype geothermometry, the reader is referred to Walker (1993) and de Caritat et al. (1993).

Geologic Setting

The Lower Tuscaloosa Formation is an ideal sedimentary unit for the study of diagenetic Ch. Ch is abundant in Lower Tuscaloosa Formation sandstone, typically occurring as 5–10 μm thick coatings on detrital grains (Thomsen 1982). Petrographic evidence indicates that the Ch formed during early diagenesis and that it may have resulted in the preservation of abnormally high primary porosity (22% at 6600 m) by coating detrital quartz grains and inhibiting growth of quartz cement (Thomsen 1982; Wiygul and Young 1987). Porous, friable sandstone typically contains well-formed Ch grain coatings, whereas samples with poorly formed Ch coatings are usually tightly cemented by secondary quartz (Thomsen 1982).

The Tuscaloosa Formation was deposited in deltaic, shallow marine, and alluvial environments in the Gulf Coast Basin during a low sea-level stand in Late Cretaceous (Cenomanian) time (e.g., Stancliffe and Adams 1986; Hogg 1988). It is a tabular unit that strikes approximately east-west, with outcrop extending from South Carolina to Mississippi. It dips about 1° to the south beneath Louisiana and Mississippi and attains a maximum burial depth of approximately 6800 m beneath southern Louisiana (Fig. 1), thus spanning a wide temperature range (Alford 1983). Lower Tuscaloosa Formation sandstone is fine to medium grained, well sorted, and ranges from sublitharenite (Stancliffe and Adams 1986) to quartz litharenite and quartz arenite (Hamlin and Cameron 1987). Detrital clasts are predominantly quartz, but volcanic and metamorphic rock fragments compose up to 27% of the bulk volume of the rock (Berg and Cook 1968; Stancliffe and Adams 1986).

Methods

All the samples analyzed in this study from depths <6000 m were core samples provided by David R. Pevear of Exxon Production Research Company, Houston, Texas. Paula Hansley of the U.S. Geological Survey, Denver, Colorado, donated core samples from 6214 to 6216 m. The cores were sampled from 14 drill holes that penetrated Lower Tuscaloosa Formation sandstone over a wide range of burial depth (1702–6216 m) (Fig. 1). The temperature interval represented by these samples is approximately 80–175 °C (Alford 1983). Most of the samples are porous, friable sandstone, but a few are well-cemented, fine-grained sandstone. The cores were washed in distilled water to remove drilling by-products and crushed in an iron mortar and pestle without grinding (Bailey 1988b). The powdered sample was immersed in distilled water and agitated for 12 h in a sample shaker. The <0.5 and 0.5–2 μm (esd) fractions were then separated by repeated centrifugation and analyzed for mixed layering, polytypism, and compositional variation in Sp-Ch.

Oriented powder aggregates were made by concentrating 50–100 mg of clay in distilled water and dropping the clay slurry onto glass slides (2.7 × 4.6 cm). XRD patterns of air-dried and ethylene glycol–solvated oriented mounts were recorded between 2 and 35° 2θ with 0.05° steps and 5 s counts to analyze the mineral content of the clay-size fractions. XRD data were obtained using an automated Siemens D-500 diffractometer with Cu$K\alpha$ radiation (40 kV and 40 mA), a graphite monochromator, and a Databox microcomputer.

The proportion of Sp layers in mixed-layer Sp-Ch was determined by the method of Reynolds et al. (1992) and verified by comparison with calculated NEWMOD diffraction patterns (Reynolds 1985). A 1° divergence slit was used in conjunction with a 0.05° aperture slit and two 2° soller slits (Reynolds et al. 1992). The Ch 004 and 005 peaks were scanned, air-dried, with 0.05° steps and count times ranging from 20 to 60 s. Analytical 004 and 005 peaks were fitted to pseudo-Voigt functions by a least-squares method, and peak breadth (β) was measured at one-half height. Interstratification of 7 Å (Sp-like) layers and 14 Å (Ch) layers can be difficult to detect because d_{001}Ch $\approx 2d_{001}$Sp, and Sp peaks essentially overlap with even-order Ch peaks. However, random interstratification of Sp and Ch causes broadening of the odd-order Ch peaks proportional to the amount of 7 Å material, making Sp-Ch interstratification identifiable and quantifiable (Reynolds et al. 1992). Accordingly, residual line broadening (β_r) caused by interstratified 7 Å Sp layers and 14 Å Ch layers was determined by the equation

$$\beta_r = (\beta_{005}^{1.25} - \beta_{004}^{1.25})^{(1/1.25)}$$

(Reynolds et al. 1992), where β_{004} and β_{005} are the peak widths at one-half height (in degrees 2θ) for the Ch 004 and 005 peaks. Instrumental distortion of the Ch 004 and 005 peaks is assumed to be very similar and thus negligible in these calculations. The percentage of Sp was determined by the empirical equation (Reynolds et al. 1992) %Sp = $-0.51 + 24.27\beta_r$. Duplicate analyses and comparisons with NEWMOD calculated patterns indicate that this method produces results that are accurate to within approximately 5% of the reported value.

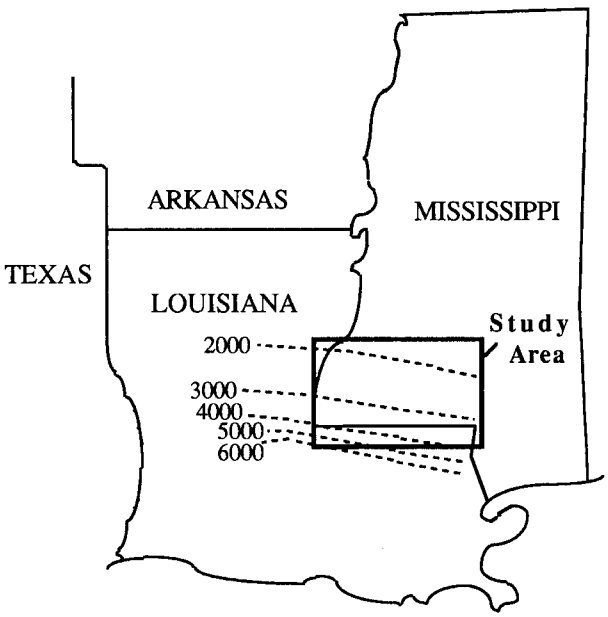

Figure 1. Location map of well sites that produced the core samples studied (after Berg and Cook 1968; Hogg 1988). Dashed lines and numbers indicate depth isopachs to the base of the Lower Tuscaloosa Formation (in meters).

To determine polytypism of Sp-Ch, random powder mounts were prepared by freeze-drying solutions of approximately 1 g of powder in 50–100 mL of distilled water. The freeze-dried powders were packed into side-loaded sample holders to maximize random orientation of the clay crystals for XRD analysis of polytypes (Reynolds 1992). The random powder mounts were scanned from 32 to 64° 2θ with 0.05° steps and count times of 15 to 20 s per step. The differential X-ray diffraction method of Schulze (1982) was used to remove illite, anatase, and kaolinite interference. This method records an initial XRD scan of the Ch-, illite-, and kaolinite-bearing random powder mount over the 2θ range of interest. The powder is then heated in warm (80 °C) 1 *N* HCl for 1 h, which destroys Fe-rich Ch (Brindley 1961). An XRD trace of the HCl-treated residual containing illite, anatase, and kaolinite is then made over the same 2θ range, after which the HCl-treated XRD pattern is digitally subtracted from the initial scan to give a Ch pattern (Fig. 2).

Ch and Sp polytypes were identified by comparison with published patterns (Brown and Bailey 1962; Bailey 1969, 1988b) and calculated patterns (Reynolds 1993). The proportion of I*bb* polytype layers in mixed-layer I*bb*-I*aa* was determined by comparing analytical XRD pat-

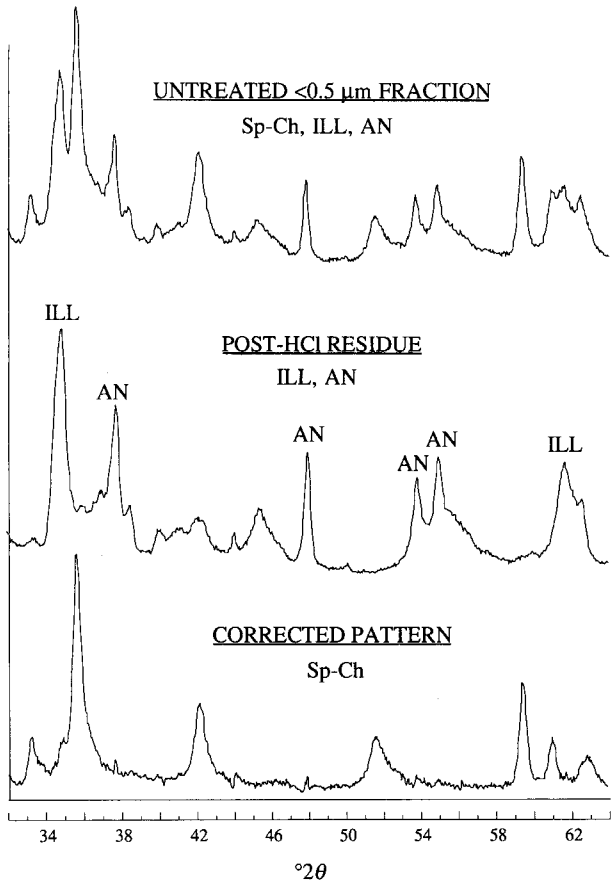

FIGURE 2. An example of differential X-ray diffraction. Sp-Ch = serpentine-chlorite, ILL = illite, and An = anatase.

terns with calculated XRD patterns (Reynolds 1993). Atomic coordinates for the calculated I*bb* structure are from Shirozu and Bailey (1965), and I*aa* coordinates were derived from the I*bb* coordinates of Shirozu and Bailey (1965) by shifting octahedral layers $\pm a/3$ relative to adjacent tetrahedral layers.

The terminology for describing mixed-layer proportions is that used by Reynolds (1988). I*bb*(0.65)-I*aa* represents a mixed-layer I*bb*-I*aa* polytype with 65% I*bb* layers. Similarly, Sp(0.15)-Ch is mixed-layer Sp-Ch with 15% Sp layers.

Scanning electron microscopy (SEM) and optical microscopy were used to determine textures, including the distribution and morphology of diagenetic Sp-Ch and the relative proportions of other diagenetic phases and detrital grain composition. Sp-Ch morphologies (e.g., grain coatings, peloids, infillings, pore fillings, and replacements) were verified by energy-dispersive X-ray (EDX) spot analysis. SEM and EDX instrumentation and operating conditions are given below.

The chemical composition of Sp-Ch from four samples (1937, 3878, 4054, and 5470 m) was determined by EDX spot analysis. Between eight and 11 EDX analyses were performed on each sample. These four samples span the range of composition with respect to polytypism and interstratified Sp. The sample from 4054 m is silty and well cemented by secondary quartz, whereas the other three are porous, friable sandstone. For SEM and EDX analyses, polished sections were coated with carbon and examined in a Zeiss DSM 962 SEM instrument with an EDX analyzer at the Dartmouth College Electron Microscope Laboratory. Samples were analyzed for FeO, MgO, Al_2O_3, SiO_2, MnO, K_2O, Na_2O, CaO, TiO_2, and P_2O_5, and analyses were normalized to a Ch unit cell with $O_{10}(OH)_8$. The compositions of 2:1 octahedral layers and hydroxide interlayer octahedral layers are assumed to be identical. Standards were pure oxides for every element except Na, for which albite was used. Biotite and a granite glass were also analyzed as secondary standards to check reliability. The accelerating voltage was 15 kV, the beam current was 6 nA, spot size was 1–2 μm, and the counting time was 100 s per analysis. The spot size of 1–2 μm is smaller than the thickness of Sp-Ch rims (5–10 μm) and significantly smaller than the size of peloids and infillings (25–50 μm), and so we are confident that the EDX analyses are relatively free of contamination from other minerals. However, intergrowths of other authigenic minerals, particularly illite, have been known to contaminate analyses (e.g., Whittle 1986; Jiang et al. 1994). Thus, all analyses with >0.5% K_2O were discarded to avoid illite contamination (Hillier 1994). All Fe was assumed to be Fe^{2+}, and Ti was excluded from the Sp-Ch structural formulas because (1) it occurs in trace quantities in most samples, and (2) it probably occurs as anatase (TiO_2). Analyses with significant amounts of TiO_2 are assumed to be intergrowths of Sp-Ch and anatase. Na, Ca, and P are also not included in structural formulas because they are present only in traces (typically less than one standard deviation) and probably occur in halite, carbonate, and apatite.

The ratio of Sp-Ch to kaolinite was estimated by comparing peak areas of the Sp-Ch 006 and kaolinite 003 peaks obtained from analytical XRD scans with corresponding peak areas determined from calculated NEWMOD patterns (Reynolds 1985). Quantitative estimates were based on XRD patterns of oriented, <2 μm fraction powders, and to minimize size segregation in the quantitative estimates, powders were mounted onto glass slides by the filter-peel method (Drever 1973; Reynolds 1992).

RESULTS

Bulk mineral content

Sp-Ch, illite, kaolinite, and anatase are present in all samples. The ratios of Sp-Ch to anatase and illite to anatase are relatively consistent and show no systematic variation, suggesting that the amounts of Sp-Ch, illite, and anatase remain relatively constant. The amount of kaolinite, however, decreases with increasing burial depth. At 1702 m burial depth, kaolinite makes up about 80% of the <2 μm fraction, whereas between 1714 and 3600 m, the <2 μm fraction contains 30–40% kaolinite, and

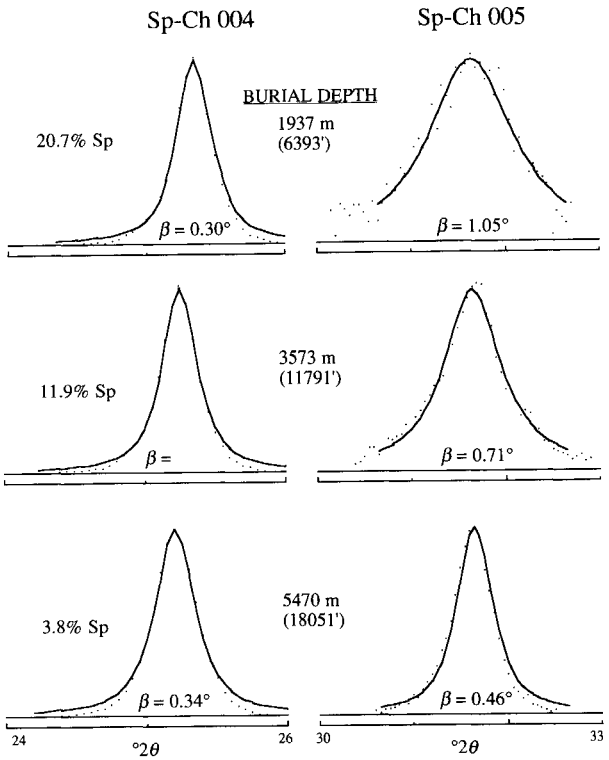

FIGURE 3. The 004 and 005 peaks of Sp-Ch. Dots are experimental points and solid lines are least-squares–fitted pseudo-Voigt profiles. Note the decrease in peak breadth (β) of the Sp-Ch 005 with increasing depth.

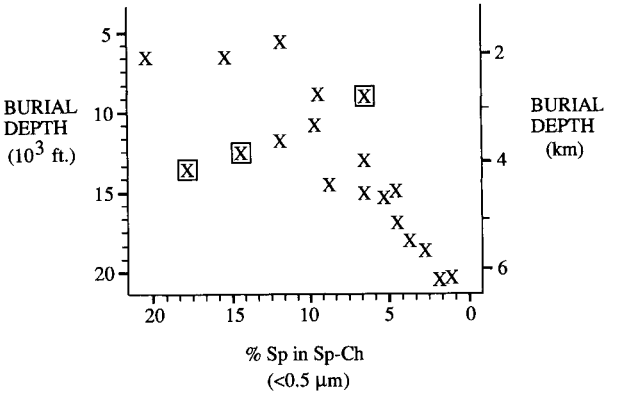

FIGURE 4. Relationship between burial depth and Sp content in mixed-layer Sp-Ch in the <0.5 μm fraction. Boxes indicate well-cemented, fine-grained specimens.

at depths greater than 3600 m, kaolinite makes up <10% of the <2 μm fraction. Weak calcite peaks were evident in some samples, reflecting the presence of fossil fragments, calcite cement, or both. Thin-section analysis showed that hematite and pyrite are present in all samples; hematite is prevalent in shallow samples, and its content decreases with burial depth, whereas the proportion of pyrite increases with burial. In some shallow samples (<2000 m), hematite occurs as grain coatings.

Texture

Thin-section studies show that in samples from <3600 m, Sp-Ch occurs as subequal combinations of grain coatings, pore fillings, peloids, and infillings. With increasing burial depth, Sp-Ch grain coatings generally increase in continuity and thickness, whereas the peloids and infillings appear to decrease in abundance. Sp-Ch in deep samples (>3600 m) most commonly occurs as prevalent, well-formed isopachous rims on detrital grains; pore fillings, peloids, and infillings are less common in the deep samples. In the 4054 m sample we found two ribbonlike occurrences of Sp-Ch that may be pseudomorphous after biotite.

In all cases, Sp-Ch grain coatings appear to have predated kaolinite and illite, and in samples that contain carbonate cement, Sp-Ch grain coatings apparently preceded the carbonate cement. Samples from <2000 m contain localized hematite grain coatings and Sp-Ch grain coatings. Quartz cement is very minor or absent in most samples, although one of the intermediate depth samples (3573 m) contains euhedral quartz overgrowths interspersed with discontinuous Sp-Ch grain coatings. In addition, the five samples that exhibit poorly developed or absent Sp-Ch rims contain abundant quartz or carbonate cement (burial depths = 2732, 2782, 3765, 4054, and 4056 m). In hand sample, these samples are fine grained and well cemented, and XRD analyses indicate that they are characterized by a Sp:Ch ratio or polytype composition (or both) that is not consistent with the general trends.

Structure

All Ch analyzed in this study contains broad odd-order 00*l* peaks, indicating the occurrence of randomly interstratified Sp-Ch in all samples (Fig. 3). In the <0.5 μm fraction, peak width at one-half height of the Sp-Ch 005 peak (β_{005}) decreases from 1.05 to 0.40° 2θ between 1702 and 6216 m burial depth, whereas β_{004} is relatively constant (0.29–0.38° 2θ) throughout the sequence (Fig. 3). The decrease in β_{005} with increasing burial reflects a decrease in the proportion of Sp layers in mixed-layer Sp-Ch from a maximum of 20.7 ± 1.1% at 1937 m to a minimum of 1.3 ± 0.1% at 6214 m (Fig. 4). In all samples, β_{004} values of Sp-Ch for the 0.5–2 μm fraction (0.22–0.33° 2θ) are less than β_{004} values for the <0.5 μm fraction (0.29 to 0.38° 2θ), indicating that mean crystallite size is greater in the coarser fraction. The percentage of Sp in Sp-Ch does not differ significantly between the two size fractions. Variations in β_{004} with depth are discussed below.

Nearly all Sp-Ch analyzed in this study contains randomly interstratified I*bb* and I*aa* layers (Fig. 5). At depths <2000 m, the polytype is essentially I*bb* (Brown and Bailey 1962), although the diminished intensity ratio of the 202:060 peaks may indicate traces of interstratified I*aa* (Fig. 5a). Composite peaks between the pure I*bb* and pure I*aa* polytype peaks are found in deeper samples, and cal-

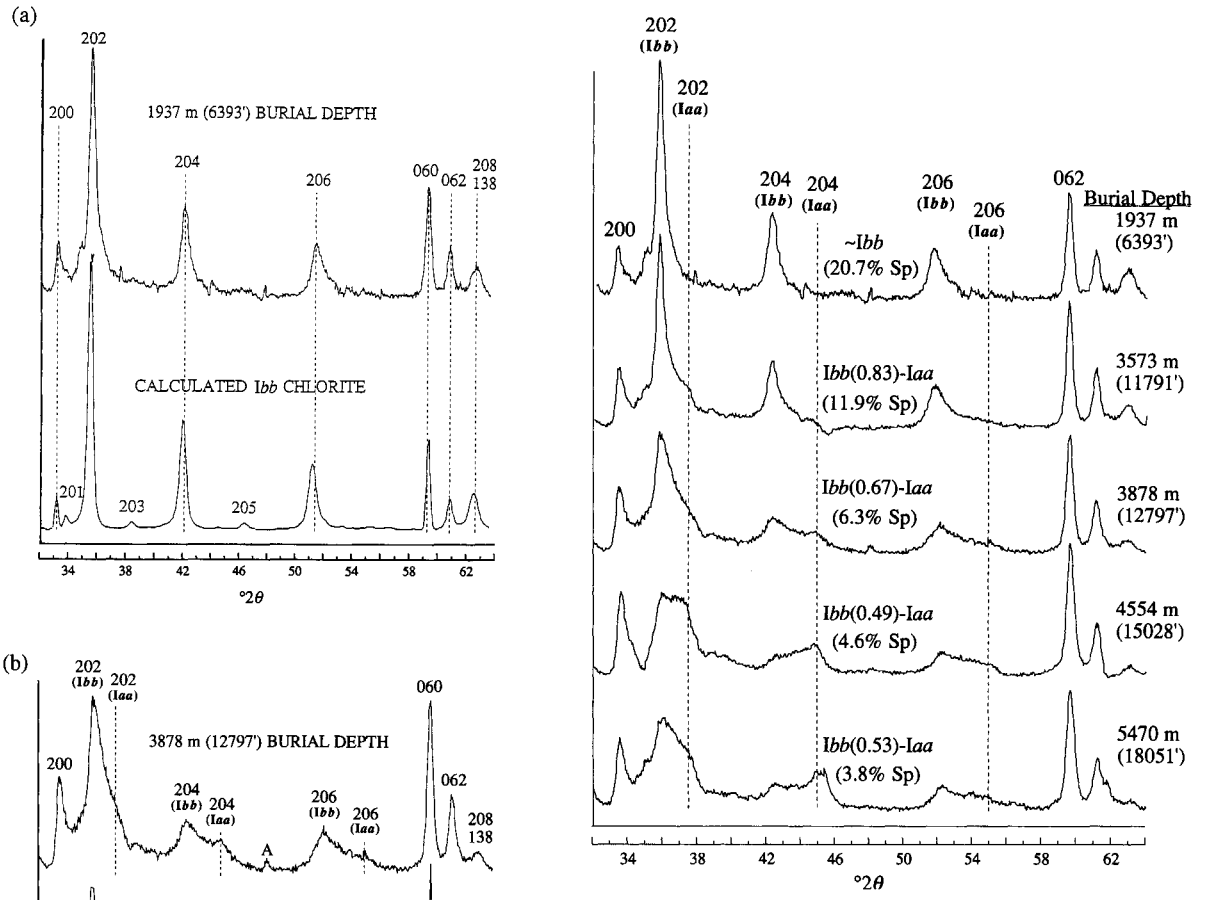

FIGURE 6. Randomly oriented XRD patterns of *Ibb*-*Iaa* polytypes showing decrease in *Ibb* component with increasing depth.

culated XRD patterns of randomly interstratified *Ibb*-*Iaa* closely match the analytical patterns (Figs. 5b and 5c). Comparison of analytical and calculated patterns shows that the *Ibb* component decreases from ~100 to 49% over the interval studied (Figs. 6 and 7). There is essentially no difference in polytype composition between the <0.5 and 0.5–2 μm fractions. The percentage of Sp in Sp-Ch is proportional to *Ibb* content in *Ibb*-*Iaa*, whereas the percentage of *Ibb* and even-order peak breadth (β_{004}) vary inversely (the percentage of *Iaa* in *Ibb*-*Iaa* is proportional to β_{004}) (Fig. 8).

The value of d_{060} systematically decreases with increasing burial from 1.556 Å in nearly pure *Ibb* to 1.549 Å in *Ibb*(0.49)-*Iaa*, as does d_{200} (2.698–2.665 Å). Measured d_{001} progressively increases with increasing burial from 14.11 to 14.16 Å, and peak breadth at one-half height of the 0 0 10 peak simultaneously increases from 0.37° 2θ in

←

FIGURE 5. Comparison of calculated diffraction patterns of polytypes (Reynolds 1993) and randomly oriented mounts: (**a**) *Ibb*, (**b**) *Ibb*(0.67)/*Iaa*, (**c**) *Ibb*(0.49)/*Iaa*. Characteristic *hkl* peaks of the pure *Ibb* and *Iaa* polytypes are shown. A = anatase.

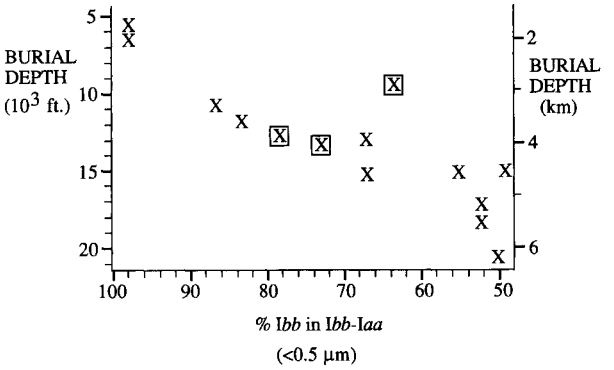

FIGURE 7. Relationship between burial depth and polytypism, <0.5 μm fraction. Boxes indicate well-cemented, fine-grained specimens.

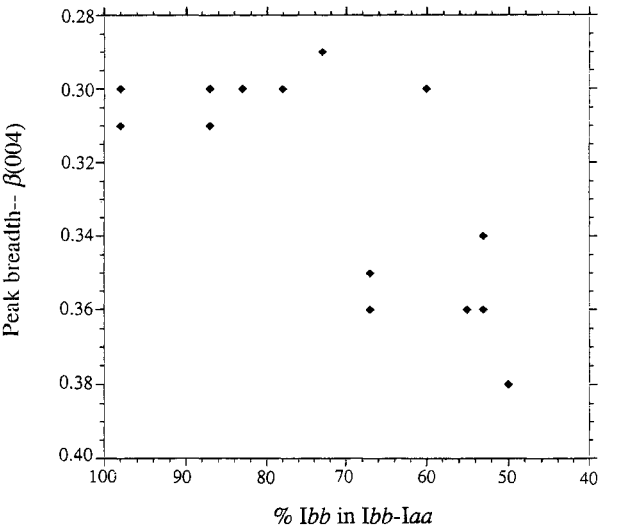

FIGURE 8. Relationship between polytypism and even-order Sp-Ch peak breadth (β_{004}).

nearly pure I*bb* to 0.56° 2θ in I*bb*(0.49)-I*aa*, suggesting that the values of d_{001} for the I*bb* and I*aa* phases are not the same. The value of d_{001} for the I*bb* phase, measured from XRD patterns, is 14.11 Å. The value of d_{001} for the I*aa* component could not be directly measured from XRD patterns (it makes up ≤51% of the I*bb*-I*aa*), and so we used NEWMOD to model broadening and migration of the 0 0 10 peak caused by interstratification of two phases with different d_{001}. Using this method, we find that d_{001} of the I*aa* phase is 14.35 Å.

Decreasing 00*l* peak breath is primarily an indicator of increasing crystallite thickness in clay minerals and is often used to interpret crystal growth during diagenesis and low-grade metamorphism (Kubler 1964; Frey 1970; Eberl et al. 1990; Hillier 1994). In Tuscaloosa Formation Sp-Ch, there is no increase in crystallite thickness (along *c**) with increasing depth, and peak breadth (β_{004}) actually increases slightly with increasing burial (Fig. 3). We attribute the increase in β_{004} to interstratification of 14.11 Å I*bb* and 14.35 Å I*aa* phases. The increase in β_{004} parallels decreasing I*bb* component (in I*bb*-I*aa*), and crystallite thickness appears to be nearly constant throughout the sequence.

Chemical composition

SEM and EDX results are presented as oxides in Table 1 and as Sp-Ch structural formulas in Table 2. In all cases, oxide totals are less than the expected 85–88% for Ch with an $O_{10}(OH)_8$ unit cell, a common problem for Ch and mixed-layer Ch minerals (e.g., Sp-Ch and corrensite). Hillier (1994) attributed low oxide totals obtained by microprobe analyses to microporosity between Ch grains, and to test whether or not low oxide totals adversely affect structural formulas, he compared a standard metamorphic Ch (CCa-1, available from the Clay Minerals Society) prepared as a polished section to the same specimen prepared as a polished 2–5 μm powder and epoxy resin mixture. The mean oxide total for the polished section was 86%, whereas the mean oxide total for the epoxy-powder section was 54%, with many totals between 20 and 50%. Although dispersion about the mean was greater for the low-oxide data, the average structural formulas obtained from the polished section and the epoxy section were nearly identical, suggesting that errors resulting from low oxide totals are random and that mean values provide reliable results.

Standard deviations associated with SEM and EDX analyses of Sp-Ch in this study were generally low: 0.8–1.1% for Si and Al, 1.0–1.5% for Fe, and 1.9–4.3% for Mg. Analytical errors were greatest for Sp-Ch from 1937 m, in which weight percent oxide totals were much less than in deeper samples. The low oxide values in the shallowest sample may be due to a greater amount of micropore space between Sp-Ch crystals that is not so pronounced at greater depths.

The high amount of TiO_2 at 1937 m (1.05%) and the elevated TiO_2 value at 3878 m (0.36%) are attributed to intergrowths of anatase and Sp-Ch in pore fillings. Individual analyses of pore fillings contained TiO_2 values of 6.44 and 1.99% at 1937 m and 2.10 and 1.24% at 3878 m, whereas all grain coatings, peloids, infillings, and pseudomorphous replacements contained only traces of TiO_2.

DISCUSSION

Origin and occurrence of Sp-Ch

The decrease in the proportion of interstratified serpentine-like layers with increasing grade raises the possibility that Sp-Ch in the Tuscaloosa Formation originated as a 7 Å mineral that subsequently transformed to mixed-layer Sp-Ch during diagenesis. The presence of Sp-Ch peloids and infillings, combined with an inferred tropical marine depositional setting, strongly suggests that the original material was odinite, an Fe-rich 7 Å mineral that forms at the sediment-seawater interface in Recent, tropical marine sediments (Odin et al. 1988; Odin 1990). Odinite is unstable outside its environment of formation,

TABLE 1. SEM and EDX analyses (weight percent) and atoms per formula unit of Sp-Ch

Burial depth (m)	1937	3878	4054	5470
No. of analyses	9	11	9	8
SiO_2	8.99 ± 0.10	16.71 ± 0.13	17.56 ± 0.13	18.82 ± 0.14
Al_2O_3	7.50 ± 0.08	13.33 ± 0.10	14.85 ± 0.12	16.60 ± 0.13
FeO	11.76 ± 0.20	21.92 ± 0.22	25.69 ± 0.25	23.92 ± 0.26
MgO	1.49 ± 0.06	3.89 ± 0.09	3.25 ± 0.08	4.84 ± 0.09
MnO	0.05 ± 0.07	0.06 ± 0.09	0.09 ± 0.10	0.05 ± 0.10
TiO_2	1.05 ± 0.07	0.36 ± 0.06	0.10 ± 0.06	0.07 ± 0.06
K_2O	0.05 ± 0.07	0.08 ± 0.09	0.05 ± 0.07	0.04 ± 0.06
Na_2O	0.13 ± 0.07	0.29 ± 0.08	0.26 ± 0.08	0.31 ± 0.08
CaO	0.11 ± 0.05	0.14 ± 0.05	0.25 ± 0.07	0.14 ± 0.05
P_2O_5	0.05 ± 0.08	0.07 ± 0.08	0.14 ± 0.10	0.08 ± 0.09
Total	31.19	56.85	62.23	64.86
Si	2.93	2.91	2.80	2.80
$^{[4]}$Al	1.07	1.09	1.20	1.20
$^{[6]}$Al	1.78	1.58	1.60	1.72
Fe	3.14	3.18	3.43	2.98
Mg	0.72	1.00	0.77	1.05
Sum (VI)*	5.64	5.76	5.80	5.75

* Number of octahedral cations (per six sites).

and it transforms to a mixed-layer 7-14 Å phase during the first stages of diagenesis (Bailey 1988a; Odin et al. 1988). In light of this, odinite probably formed within the upper decimeter of Tuscaloosa Formation sediment soon after deposition in a tropical marine environment (Odin et al. 1988). Ultrabasic volcanic rock fragments, which are ubiquitous in the Tuscaloosa Formation (Thomsen 1982), and possibly Fe-rich river water (Odin et al. 1988), provided cations that precipitated as poorly crystallized odinite shortly after deposition. During very early diagenesis, perhaps within a few meters of the surface (Bailey 1988a), the odinite peloids and infillings dissolved and reprecipitated as Sp-Ch. This transformation resulted in the formation of Sp-Ch coatings, although some of the original odinite textures were preserved. The transformation of odinite to Sp-Ch coatings during early diagenesis is consistent with petrographic evidence indicating that Sp-Ch grain coatings preceded all other diagenetic phases with the possible exception of hematite. The early diagenetic transformation of odinite to grain-coating Ch has also been observed in Jurassic sandstones of the Norwegian continental shelf (Ehrenberg 1993).

TABLE 2. Structural formulas for different morphologies of Sp-Ch

Sp-Ch structural formula	Texture
1937 m burial depth	
$(Fe_{3.05}Mg_{0.75}Al_{1.84})(Si_{2.91}Al_{1.09})O_{10}(OH)_8$	PF (N = 2)
$(Fe_{3.01}Mg_{0.71}Al_{1.82})(Si_{3.13}Al_{0.87})O_{10}(OH)_8$	PEL (N = 2)
$(Fe_{3.40}Mg_{0.68}Al_{1.65})(Si_{2.78}Al_{1.22})O_{10}(OH)_8$	INF (N = 2)
$(Fe_{3.13}Mg_{0.74}Al_{1.79})(Si_{2.92}Al_{1.08})O_{10}(OH)_8$	GC (N = 3)
$(Fe_{3.14}Mg_{0.72}Al_{1.78})(Si_{2.93}Al_{1.07})O_{10}(OH)_8$	avg.
3878 m burial depth	
$(Fe_{3.07}Mg_{0.98}Al_{1.64})(Si_{2.96}Al_{1.04})O_{10}(OH)_8$	PF (N = 3)
$(Fe_{2.92}Mg_{1.00}Al_{1.76})(Si_{2.87}Al_{1.13})O_{10}(OH)_8$	PEL (N = 1)
$(Fe_{3.63}Mg_{0.93}Al_{1.35})(Si_{2.83}Al_{1.17})O_{10}(OH)_8$	INF (N = 2)
$(Fe_{3.12}Mg_{1.03}Al_{1.61})(Si_{2.88}Al_{1.12})O_{10}(OH)_8$	GC (N = 5)
$(Fe_{3.18}Mg_{1.00}Al_{1.58})(Si_{2.91}Al_{1.09})O_{10}(OH)_8$	avg.
4054 m burial depth	
$(Fe_{3.37}Mg_{0.72}Al_{1.65})(Si_{2.88}Al_{1.12})O_{10}(OH)_8$	PF (N = 1)
$(Fe_{3.43}Mg_{0.81}Al_{1.56})(Si_{2.80}Al_{1.20})O_{10}(OH)_8$	PEL (N = 2)
$(Fe_{3.60}Mg_{0.76}Al_{1.50})(Si_{2.78}Al_{1.22})O_{10}(OH)_8$	RPL (N = 2)
$(Fe_{3.32}Mg_{0.77}Al_{1.67})(Si_{2.81}Al_{1.19})O_{10}(OH)_8$	INF (N = 1)
$(Fe_{3.38}Mg_{0.78}Al_{1.63})(Si_{2.78}Al_{1.22})O_{10}(OH)_8$	GC (N = 3)
$(Fe_{3.43}Mg_{0.77}Al_{1.60})(Si_{2.80}Al_{1.20})O_{10}(OH)_8$	avg.
5470 m burial depth	
$(Fe_{2.85}Mg_{1.19}Al_{1.65})(Si_{2.86}Al_{1.14})O_{10}(OH)_8$	PF (N = 1)
$(Fe_{2.80}Mg_{1.07}Al_{1.80})(Si_{2.88}Al_{1.12})O_{10}(OH)_8$	INF (N = 2)
$(Fe_{3.03}Mg_{1.04}Al_{1.69})(Si_{2.77}Al_{1.23})O_{10}(OH)_8$	GC (N = 5)
$(Fe_{2.95}Mg_{1.07}Al_{1.72})(Si_{2.81}Al_{1.19})O_{10}(OH)_8$	avg.

Note: PF = pore fillings, PEL = peloids, INF = infillings, GC = grain coatings, and RPL = replacements; N = number of analyses.

The presence of mixed-layer Sp-Ch in all samples is probably due to (1) the widespread occurrence of volcanic rock fragments in Tuscaloosa Formation sandstone (Thomsen 1982; Genuise and McBride 1990) and (2) a tropical, shallow marine depositional environment that favored odinite formation (Odin 1990). Anatase, which was detected in all samples by XRD analysis, probably formed when Ti was excluded from odinite during crystallization following the dissolution of mafic fragments (cf. Eggleton and Banfield 1985), or it formed during the transformation of odinite to Sp-Ch. The coexistence of hematite and Sp-Ch indicates that conditions during Sp-Ch crystallization were slightly oxidizing and that pH was nearly neutral (Garrels and Christ 1965).

Composition

Compositions determined by SEM and EDX are relatively consistent throughout the sequence (Table 1), although infillings of Sp-Ch appear to contain more Fe and less $^{[6]}$Al than the other textures (Table 2), and Sp-Ch from 4054 m contains about 10% more Fe than the other samples. The total number of octahedral cations (per six sites) ranges from 5.6 to 5.8 and shows no systematic variation with depth. The apparent octahedral site vacancies may be due to greater amounts of $^{[6]}$Al than $^{[4]}$Al (Foster 1962; Whittle 1986), although a recent analytical electron microscope (AEM) study by Jiang et al. (1994) indicated that octahedral vacancies in Ch minerals are analytical artifacts caused by inclusions of other minerals.

Structural formulas of Tuscaloosa Formation Sp-Ch

determined by SEM and EDX in this study are very similar to both mixed-layer berthierine-chlorite sampled from Gulf Coast mudstones and analyzed by AEM (Jiang et al. 1994) and mixed-layer 7-14 Å minerals obtained from a variety of sandstones and analyzed by microprobe (Hillier 1994).

Structure of Sp-Ch

The decrease in the proportion of Sp-like layers in mixed-layer Sp-Ch with increasing burial depth indicates that Sp-like layers transform to Ch layers with increasing grade, a finding consistent with similar reports by Nelson and Roy (1958), Karpova (1969), Iijima and Matsumoto (1982), Walker and Thompson (1990), and Hillier (1994). The Sp-to-Ch transformation is essentially a polymorphic transition involving compositionally similar or identical 7 and 14 Å phases (Xu and Veblin 1993; Jiang et al. 1994). Polytypes are defined as different stacking arrangements of successive layers that are identical in both composition and structure (Moore and Reynolds 1989), and so strictly speaking, 7 Å Sp-like layers cannot be considered polytypes of 14 Å Ch layers. However, the two phases are crystallographically similar (Fig. 9), and the 7 to 14 Å transformation only requires inversion of a tetrahedral sheet (Brindley 1961; Reynolds 1988).

Previous studies have shown that both Sp and Ch occur as orthohexagonal polytypes in sandstone (e.g., Brown and Bailey 1962; Karpova 1969; Walker 1993). Karpova (1969) referred to both the orthohexagonal Sp polytype and the orthohexagonal Ch polytype as I*bb*. Bailey (1969) indexed the 1*T* Sp polytype on a *C*-centered, orthohexagonal cell. Other than the lack of 14 Å 00*l* peaks, its powder diffraction pattern is virtually identical to that of I*bb* Ch (Brown and Bailey 1962; Bailey 1969), and it is probably the same polytype referred to as I*bb* Sp by Karpova (1969). In the Tuscaloosa Formation, XRD patterns indicating the occurrence of the orthohexagonal I*bb* structure in mixed-layer Sp-Ch with 11.8–20.7% Sp layers suggest that both Sp and Ch occur as orthohexagonal polytypes. Sp most commonly occurs as an orthohexagonal polytype (Bailey 1969), and interstratification of I*bb* Ch and orthohexagonal (I*bb* or 1*T*) Sp with similar atomic geometries (Brindley 1961) would produce a good fit between adjacent layers along the basal plane. Accordingly, we conclude that the mixed-layer Sp-Ch consists of orthohexagonal (I*bb*) Sp-like layers interstratified with Ch layers of both the I*bb* and I*aa* polytypes and can be envisioned as a three-component interstratification of I*bb* Sp, I*bb* Ch, and I*aa* Ch. Shallow samples (<2000 m) are dominated by interstratified I*bb* Sp and I*bb* Ch, and the deep samples are characterized by interstratified I*aa* Ch and I*bb* Ch with minor I*bb* Sp. To our knowledge, this is the only documented occurrence of interstratified Ch polytypes.

A model for the diagenetic Sp-Ch reactions is as follows. After the early diagenetic transformation of odinite to I*bb* Sp-Ch, I*bb* Sp layers transform to I*bb* Ch layers as grade increases with progressive sedimentation and burial. At depths greater than 2000 m, some of the I*bb* layers transform to I*aa* layers, creating crystals of randomly interstratified I*bb* and I*aa* polytypes. The I*bb*-to-I*aa* transformation occurs simultaneously with the Sp-to-Ch reaction, implying that I*bb* Sp layers transform to I*aa* Ch layers at depths >2000 m. The consistent chemical composition of Sp-Ch, as determined by EDX, indicates that the reactions of I*bb* Sp to I*bb* Ch and I*bb* Sp to I*aa* Ch are isochemical and thus are polymorphic transitions (Jiang et al. 1992; Xu and Veblin 1993). This finding is similar to those of Jiang et al. (1992) and Xu and Veblin (1993), who observed isochemical 7-14 Å transformations, and Brown and Bailey (1962), who documented isochemical I*bb*-to-I*aa* transformations.

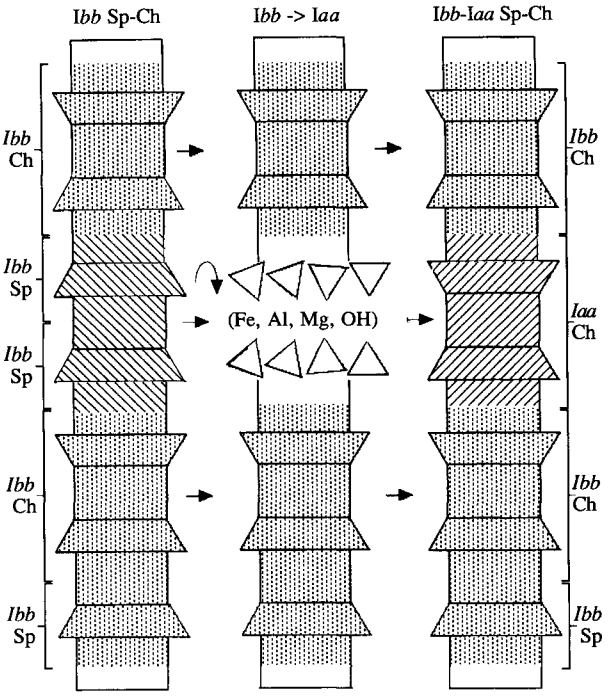

FIGURE 9. Schematic depiction of the possible I*bb* Sp–to–I*aa* Ch transformation.

An alternate interpretation of the gradual transformation of Sp layers to Ch layers with increasing burial is that all the Sp-Ch formed simultaneously during a basinwide fluid-flow event, a phenomenon that has been observed in illite-smectite of the U.S. Gulf Coast Basin (Morton 1985). During punctuated or episodic diagenesis, all minerals form simultaneously with mixed-layer proportions that reflect current burial temperatures, thus producing more evolved minerals at depth, whereas during burial diagenesis, individual layers or crystallites continually transform as temperatures increase with progressive burial, also producing more evolved minerals at depth. We conclude that the Sp-Ch reactions occurred progressively as burial depth increased on the basis of petrographic evidence indicating that (1) the Sp-Ch grain coatings formed during very early diagenesis at shallow

burial depth (Thomsen 1982), and (2) the precursor to Sp-Ch appears to be odinite, which transforms to Ch or Sp-Ch within a few meters of the surface (Bailey 1988a).

The coincidence of increasing I*aa* content and decreasing kaolinite content raises the question of whether or not kaolinite dissolution was related to formation of the I*aa* polytype. Boles and Franks (1979) found a similar relationship between kaolinite content and bulk Ch content in sandstone of the Wilcox Formation and suggested that kaolinite dissolves and combines with Fe and Mg (provided by the illitization reaction) to form Ch. In the Tuscaloosa Formation, the consistent nature of Sp-Ch crystallite thickness and the lack of systematic variation in the Sp-Ch to anatase ratio suggests that no new Sp-Ch forms upon kaolinite dissolution. However, the dissolution of kaolinite may reflect increases in either pore-water pH (Garrels and Christ 1965) or temperature that caused the transformation of I*bb* layers to I*aa* layers.

Alford (1983) and Beskin (1984) identified the II*b* Ch polytype in deeply buried Tuscaloosa Formation sandstones, as did Ryan and Reynolds (1993). However, after using differential diffraction (Schulze 1982) to remove illite and anatase interference (Fig. 2), we now believe that the presence of illite and anatase peaks with *d* values similar to those of II*b* Ch polytype peaks (e.g., $20\bar{1}$, $20\bar{2}$, and 202) led to the II*b* misinterpretation. We also magnetically separated some of the deeply buried samples (Tellier et al. 1988; Walker and Thompson 1990) and found no evidence of the II*b* Ch polytype, indicating that the differential diffraction technique did not preferentially discriminate against II*b* polytype identification.

Implications of the mineralogic reactions

The trend of increasing I*aa* component in mixed-layer I*bb*-I*aa* may represent a prograde progression from pure I*bb* to pure I*aa* through an intermediate mixed-layer I*bb*-I*aa* series. This trend is especially noteworthy when considered in conjunction with the occurrence of the I*aa* Ch at $\leq$250 °C in Appalachian shales (Weaver et al. 1984) and the prograde transformation of I*bb* to I*aa* in iron formations (Brown and Bailey 1962). It is interesting to note that there appears to be almost as many documented examples of I*bb*-to-I*aa* transformations as the expected I*b*-to-II*b* transformation (Hillier 1994; Spötl et al. 1994). Perhaps the transition from type-I to type-II Ch is inhibited by compositional differences between Fe-rich I*bb* and the more Mg-rich II*b*, or by the necessary rotation of hydroxide layers, or both (Bailey 1988b; Walker 1993).

The lack of variation in mean crystallite thickness implies that the reaction of Sp layers to Ch layers does not involve crystal-growth mechanisms typical of other common clay minerals. In illites, kaolins, and some chlorites, crystallite size commonly increases with increasing grade, reflecting simultaneous dissolution of fine-grained crystals and crystallization on coarser existing crystals (Kubler 1964; Eberl et al. 1990; Jahren 1991; Warr and Rice 1994; Hillier 1994; Spötl et al. 1994). If Sp-Ch crystals dissolved and reprecipitated during the Sp-to-Ch reaction, crystallite size should increase with increasing grade (Eberl et al. 1990), but we have not observed such a trend. Sp-Ch crystals are probably not destroyed during the reaction, and the simultaneous Sp-to-Ch and I*bb*-to-I*aa* transformations probably involve disaggregation and reorganization of individual layers on a layer-by-layer basis, a process that has been observed in transformations of biotite to Ch (Eggleton and Banfield 1985; Li and Peacor 1993) and berthierine to Ch (Ahn and Peacor 1985; Xu and Veblin 1993) and inferred for illite-smectite (Altaner and Ylagin 1993) and Sp-Ch (Ryan et al. 1994). By reacting in this manner, individual layers transform and the integrity of the existing crystal is preserved (Fig. 9).

There are distinct differences between transformations in Sp-Ch and illite. The I*bb*-to-I*aa* polytype transformation occurs simultaneously with the reaction of Sp to Ch, but in mica, nearly all smectite reacts to illite before the $1M_d$ polytype transforms to $2M_1$ (Maxwell and Hower 1967; Moe et al. 1996). The reaction of $1M_d$ to $2M_1$ illite is a dissolution-reprecipitation reaction (Reynolds 1965) that produces physical mixtures of $1M_d$ and $2M_1$, but no interstratification of $1M_d$ and $2M_1$ layers (Moe et al. 1996), whereas the I*bb*-to-I*aa* reaction produces randomly interstratified polytype layers (I*bb*-I*aa*) and does not result in crystal growth. Also, the illitization reaction requires changes in tetrahedral and interlayer composition (Hower et al. 1976), but reactions in Sp-Ch appear to be isochemical (Ahn and Peacor 1985; Jiang et al. 1992; Xu and Veblin 1993).

Relationship between Sp-Ch and porosity

Our findings support the work of many others (e.g., Heald and Anderegg 1960; Pittman and Lumsden 1968; Thomsen 1982; Ehrenberg 1993), who have indicated that the formation of chloritic grain coatings during early diagenesis is responsible for the preservation of abnormally high primary porosity. By forming during early diagenesis, the grain coatings covered potential nucleation sites and inhibited the growth of quartz cement. However, the growth of quartz cement may be influenced by grain size. At depths >3600 m, Tuscaloosa Formation sandstones that contain fine-grained quartz and detrital clay are well cemented by secondary quartz, whereas sandstones with little or no quartz cement are medium grained and contain no evidence of detrital clay. The fine-grained detrital quartz, which is more reactive than medium-grained quartz, may have dissolved and reprecipitated as cement in situ, or the high concentration of potential quartz nucleation sites in the fine-grained rocks may have fostered growth of quartz cement from solution. There is little evidence of dissolution of carbonate or framework grains, implying that most of the porosity is primary, although kaolinite dissolution may have created some secondary porosity.

Potential for Sp-Ch geothermometry

The reaction of Sp layers to Ch layers and I*bb* layers to I*aa* layers raises the possibility of Sp-Ch and I*bb*-I*aa*

geothermometry in sandstone. Grain-coating Ch is common in sandstones, especially those deposited in nearshore and shallow marine environments. Other occurrences of Sp-Ch in nearshore marine sandstones (Ahn and Peacor 1985; Walker and Thompson 1990; Hillier and Velde 1992; Hillier 1994) may be intermediates in similar mixed-layer series, indicating that the use of such a geothermometer could be widely applied. Sp-Ch is more common than illite-smectite in some sandstones, and a Sp-Ch geothermometer could be more useful at higher diagenetic grades than illite-smectite. The reactions of Sp-to-Ch and I*bb*-to-I*aa* polytype appear to be isochemical, suggesting that temperature is the dominant control on the reactions.

Scatter in the Sp-to-Ch trend may indicate that temperature is not the only controlling factor on Sp-Ch structure, but some of the scatter appears to be related to rock type. The three samples that are most anomalous with respect to Sp content and polytype composition are fine grained, silty, and well cemented, whereas all other samples analyzed in this study are medium grained and friable. The presence of detrital clays in the anomalous samples may have created a different environment (e.g., chemistry, pressure, permeability) in the fine-grained sandstones and siltstones than that present in the coarser sandstones. However, even discounting the three fine-grained samples, there is still scatter in the Sp-to-Ch and I*bb*-to-I*aa* trends, suggesting that factors other than temperature are involved in the Sp-to-Ch and I*bb*-to-I*aa* reactions. Sp layers may form metastably in the field of Ch (Jiang et al. 1992; Bailey et al. 1995), and both I*bb* and I*aa* may form metastably in the field of II*b* Ch (Bailey 1988b), indicating that the reactions observed here may be partially controlled by kinetic factors.

Thus, although it appears that temperature is the dominant control on the Sp-Ch and I*bb*-I*aa* reactions, strict interpretation of temperature on the basis of Sp:Ch ratio, I*bb*:I*aa* ratio, or both must be approached with caution. The proportions of Sp layers in Sp-Ch and I*bb* layers in I*bb*-I*aa* would probably be best used as estimates of relative diagenetic grade rather than absolute temperature. The reader is referred to articles by Walker (1993), de Caritat et al. (1993), and Jiang et al. (1994) for discussions on some of the problems inherent in clay mineral geothermometry.

Acknowledgments

Constructive reviews by Donald Peacor and Jeffrey Walker greatly improved this paper, as did an earlier review by Jeffrey Moe. We appreciate the support of David R. Pevear of Exxon Production Research Company, Houston, Texas, who provided core samples, thin sections, and financial support, and also Paula Hansley, U.S. Geological Survey, Denver, Colorado, for providing core samples from 6214 to 6216 m depth. Joel Blum and Melody Brown of the Dartmouth College Earth Sciences Department assisted with SEM analyses, as did Charles Daghlian and Louisa Howard of the Dartmouth College Electron Microscope Lab. Libby Stern is thanked for helpful discussions and for sending files to P.C.R. in Montana. Polished sections used in SEM and EDX analyses were prepared by Mineral Optics Laboratory of Wilder, Vermont.

References cited

Ahn, J.H., and Peacor, D.R. (1985) Transmission electron microscopic study of diagenetic chlorite in Gulf Coast argillaceous sediments. Clays and Clay Minerals, 33, 228–237.

Alford, E.V. (1983) Compositional variations of authigenic chlorites in the Tuscaloosa Formation, Upper Cretaceous of the Gulf Coast Basin. M.S. thesis, University of New Orleans, Louisiana.

Altaner, S.P., and Ylagin, R.F. (1993) Interlayer-by-interlayer dissolution: A new mechanism for smectite illitization. Programs and Abstracts, 30th Annual Meeting of the Clay Minerals Society, San Diego, California, 88.

Bailey, S.W. (1969) Polytypism of trioctahedral 1:1 layer silicates. Clays and Clay Minerals, 17, 355–371.

——— (1988a) Odinite, a new dioctahedral-trioctahedral Fe^{3+}-rich 1:1 clay mineral. Clay Minerals, 23, 237–247.

——— (1988b) Chlorites: Structures and crystal chemistry. In Mineralogical Society of America Reviews in Mineralogy, 19, 347–403.

Bailey, S.W., Banfield, J.F., Barker, W.W., and Katchan, G. (1995) Dozyite, a 1:1 regular interstratification of serpentine and chlorite. American Mineralogist, 80, 65–77.

Berg, R.R., and Cook, B.C. (1968) Petrology and origin of Lower Tuscaloosa sandstones, Mallalieu Field, Lincoln County, Mississippi. Transactions—Gulf Coast Association of Geological Societies, 10, 207–213.

Beskin, E.A. (1984) Compositional variations of authigenic chlorites in the Tuscaloosa Formation, Upper Cretaceous, of the Gulf Coast Basin. Programs and Abstracts, 21st Annual Meeting of the Clay Minerals Society, Baton Rouge, Louisiana, 25.

Bhattacharyya, D.P. (1983) Origin of berthierine in ironstones. Clays and Clay Minerals, 31, 173–182.

Boles, J.R., and Franks, S.G. (1979) Clay diagenesis in Wilcox sandstones of southwest Texas: Implications of smectite diagenesis on sandstone cementation. Journal of Sedimentary Petrology, 49, 55–70.

Brindley, G.W. (1961) Chlorite minerals. In G. Brown, Ed., The X-ray identification and crystal structures of clay minerals, p. 242–296. Mineralogical Society, London, U.K.

Brindley, G.W., and Gillery, F.H. (1954) Mixed-layer kaolinite-chlorite. Clays and Clay Minerals, 2nd National Conference, 349–353.

Brown, B.E., and Bailey, S.W. (1962) Chlorite polytypism: I. Regular and semi-random one-layer structures. American Mineralogist, 47, 819–850.

Burton, J.H., Krinsley, D.H., and Pye, K. (1987) Authigenesis of kaolinite and chlorite in Texas Gulf Coast sediments. Clays and Clay Minerals, 35, 291–296.

Dean, R.S. (1983) Authigenic trioctahedral clay minerals coating Clearwater Formation sand grains at Cold Lake, Alberta, Canada. Programs and Abstracts, 20th Annual Meeting of the Clay Minerals Society, Buffalo, New York, 79.

de Caritat, P., Hutcheon, I., and Walshe, J.L. (1993) Chlorite geothermometry: A review. Clays and Clay Minerals, 41, 219–239.

Drever, J.I. (1973) The preparation of oriented clay mineral specimens for X-ray diffraction analysis by a filter-membrane peel technique. American Mineralogist, 58, 553–554.

Eberl, D.D., Srodon, J., Kralik, M., Taylor, B.E., and Peterman, Z.E. (1990) Ostwald ripening of clays and metamorphic minerals. Science, 248, 474–477.

Eggleton, R.A., and Banfield, J.F. (1985) The alteration of granitic biotite to chlorite. American Mineralogist, 70, 902–910.

Ehrenberg, S.N. (1993) Preservation of anomalously high porosity in deeply buried sandstones by grain-coating chlorite: Examples from the Norwegian Continental Shelf. American Association of Petroleum Geologists Bulletin, 77, 1260–1286.

Foster, M.D. (1962) Interpretation of the composition and classification of the chlorites. U.S. Geological Survey Professional Paper 414-A, 1–33.

Frey, M. (1970) The step from diagenesis to metamorphism in pelitic rocks during alpine orogenesis. Sedimentology, 15, 261–279.

Garrels, R.M., and Christ, C.L. (1965) Solutions, minerals, and equilibria, 450 p. Harper and Row, New York.

Genuise, J.J., and McBride, E.F. (1990) SEM petrography and XRD analysis of authigenic chlorite in Oligocene and Cretaceous sandstones of

the Texas/Louisiana Gulf Coast. Programs and Abstracts, 27th Annual Meeting of the Clay Minerals Society, Columbia, Missouri, 51.

Hamlin, K.H., and Cameron, C.P. (1987) Sandstone petrology and diagenesis of Lower Tuscaloosa Formation reservoirs in the McComb and Little Creek field areas, southwest Mississippi. Transactions—Gulf Coast Association of Geological Societies, 37, 95–104.

Hayes, J.B. (1970) Polytypism of chlorite in sedimentary rocks. Clays and Clay Minerals, 18, 285–306.

Heald, M.T., and Anderegg, R.C. (1960) Differential cementation in the Tuscarora sandstone. Journal of Sedimentary Petrology, 30, 568–577.

Hillier, S. (1993) Origin, diagenesis, and mineralogy of chlorite minerals in Devonian lacustrine mudrocks, Orcadian Basin, Scotland. Clays and Clay Minerals, 41, 240–259.

——— (1994) Pore-lining chlorites in siliciclastic reservoir sandstones: Electron microscope, SEM, and XRD data, and implications for their origin. Clay Minerals, 29, 665–679.

Hillier, S., and Velde, B. (1992) Chlorite interstratified with a 7 Å mineral: An example from offshore Norway and possible implications for the interpretation of the composition of diagenetic chlorites. Clay Minerals, 27, 475–486.

Hogg, M.D. (1988) Newtonia Field: A model for mid-dip Lower Tuscaloosa retrograde deltaic sedimentation. Transactions—Gulf Coast Association of Geological Societies, 38, 461–471.

Hower, J., Eslinger, E.V., Hower, M.E., and Perry, E.A. (1976) Mechanism of burial metamorphism of argillaceous sediments. Geological Society of America Bulletin, 87, 725–737.

Iijima, A., and Matsumoto, R. (1982) Berthierine and chamosite in coal measures of Japan. Clays and Clay Minerals, 30, 264–274.

Jahren, J.S. (1991) Evidence of Ostwald ripening related recrystallization of diagenetic chlorites from reservoir rocks offshore Norway. Clay Minerals, 26, 169–178.

Jiang, W.-T., Peacor, D.R., and Slack, J.F. (1992) Microstructures, mixed-layering, and polymorphism of chlorite and retrograde berthierine in the Kidd Creek massive sulfide deposit, Ontario. Clays and Clay Minerals, 40, 501–514.

Jiang, W.-T., Peacor, D.R., and Buseck, P.R. (1994) Chlorite geothermometry? Contamination and apparent octahedral vacancies. Clays and Clay Minerals, 42, 593–605.

Karpova, G.V. (1969) Clay mineral post-sedimentary ranks in terrigenous rocks. Sedimentology, 13, 5–20.

Kubler, B. (1964) Les argiles, indicateurs de metamorphisme. Revue, Institut Francais du Petrole, 19, 1093–1112.

Li, G., and Peacor, D.R. (1993) Sulfides precipitated in chlorite altered from detrital biotite: A mechanism for local sulfate reduction? Abstracts with Programs, 105th Annual Meeting of the Geological Society of America, Boston, Massachusetts, 25, 146–147.

Maxwell, D.T., and Hower, J. (1967) High-grade diagenesis and low-grade metamorphism of illite in the Precambrian Belt Series. American Mineralogist, 52, 843–856.

Moe, J.A., Ryan, P.C., Elliott, W.C., and Reynolds, R.C., Jr. (1996) The mineralogy, chemistry, and K-Ar dating of a K-bentonite in the Proterozoic Belt Supergroup, Montana. Journal of Sedimentary Research, in press.

Moore, D.M., and Reynolds, R.C., Jr. (1989) X-ray diffraction and the identification and analysis of clay minerals, 332 p. Oxford University Press, New York.

Moore, D.M., and Hughes, R.E. (1990) The clay mineralogy of two Mississippian sandstone reservoirs in the Illinois Basin. Programs and Abstracts, 27th Annual Meeting of the Clay Minerals Society, Columbia, Missouri, 90.

——— (1991) Characteristics of chlorite interlayered with a 7Å mineral as found in sandstone reservoirs (abs.). Programs and Abstracts, Clay Minerals Society, 28, 115.

Morton, J.P. (1985) Rb-Sr evidence for punctuated illite/smectite diagenesis in the Oligocene Frio Formation, Texas Gulf Coast. Geological Society of America Bulletin, 96, 114–122.

Nelson, B.W., and Roy, R. (1958) Synthesis of the chlorites and their structural and chemical constitution. American Mineralogist, 43, 707–725.

Odin, G.S. (1985) La "verdine," facies granulaire vert, marin et cotier distinct de la glauconie: Distribution actuelle et composition. Compte Rendus de l'Académie des Sciences de Paris, 301, II(2), 105–118.

——— (1990) Clay mineral formation at the continent-ocean boundary: The verdine facies. Clay Minerals, 25, 477–483.

Odin, G.S., Bailey, S.W., Amouric, M., Frolich F., and Waychunas, G.S. (1988) Mineralogy of the verdine facies. In Developments in Sedimentology, 45, 159–206.

Pittman, E.D., and Lumsden, D.N. (1968) Relationship between chlorite coatings on quartz grains and porosity, Spiro Sand, Oklahoma. Journal of Sedimentary Petrology, 38, 668–670.

Reynolds, R.C., Jr. (1965) Geochemical behaviour of boron during the metamorphism of carbonate rocks. Geochimica et Cosmochimica Acta, 29, 1101–1113.

——— (1985) NEWMOD: A computer program for the calculation of one-dimensional diffraction profiles of clays. Hanover, New Hampshire.

——— (1988) Mixed layer chlorite minerals. In S.W. Bailey, Ed., Hydrous Phyllosilicates (Exclusive of Micas), Reviews in Mineralogy, 19, 601–629. Mineralogical Society of America, Washington, D.C.

——— (1992) X-ray diffraction studies of illite/smectite from rocks, <1 μm randomly oriented powders, and <1 μm oriented powder aggregates: The absence of laboratory-induced artifacts. Clays and Clay Minerals, 40, 387–398.

——— (1993) WILDFIRE—A computer program for the calculation of three-dimensional diffraction profiles of clays. Hanover, New Hampshire.

Reynolds, R.C., Jr., DiStefano, M.P., and Lahann, R.W. (1992) Randomly interstratified serpentine/chlorite: Its detection and quantification by powder X-ray diffraction methods. Clays and Clay Minerals, 40, 262–267.

Ruotsala, A.P., Pfluger, C.E., and Dow, G.M. (1964) Iron-rich serpentine and chamosite from Ely, Minnesota. American Mineralogist, 49, 993–1001.

Ryan, P.C., and Thompson, G.R. (1991) Structural and compositional variations in low-grade metamorphic illite and chlorite from the Belt Supergroup, Montana and Idaho. Programs and Abstracts, 28th Annual Meeting of the Clay Minerals Society, Houston, Texas, 134.

Ryan, P.C., and Reynolds, R.C., Jr. (1993) Diagenesis of chlorite in sandstone of the Gulf Coast Tuscaloosa Formation. Programs and Abstracts, 30th Annual Meeting of the Clay Minerals Society, San Diego, California, 87.

Ryan, P.C., Chamberlain, C.P., Conrad, M.E., and Reynolds, R.C., Jr. (1994) Stable isotopic implications for diagenetic mineral reactions in Tuscaloosa Formation sandstone. Programs and Abstracts, 31st Annual Meeting of the Clay Minerals Society, Saskatoon, Saskatchewan, 78.

Schulze, D.G. (1982) The identification of soil iron oxide minerals by differential X-ray diffraction. Soil Science Society of America Journal, 45, 437–440.

Shirozu, H., and Bailey, S.W. (1965) Chlorite polytypism: III. Crystal structure of an orthohexagonal iron chlorite. American Mineralogist, 50, 868–885.

Slack, J.F., Jiang, W.-T., Peacor, D.R., and Okita, P.M. (1992) Hydrothermal and metamorphic berthierine from the Kidd Creek volcanogenic massive sulfide deposit, Timmins, Ontario. Canadian Mineralogist, 30, 1127–1142.

Spötl, C., Houseknecht, D.W., and Longstaffe, F.J. (1994) Authigenic chlorites in sandstones as indicators of high-temperature diagenesis, Arkoma Foreland Basin, USA. Journal of Sedimentary Research, A64, 553–566.

Stancliffe, R.J., and Adams, E.R. (1986) Lower Tuscaloosa fluvial channel styles at Liberty Field, Amite County, Mississippi. Transactions—Gulf Coast Association of Geological Societies, 36, 305–313.

Tellier, K.E., Hluchy, M.M., Walker, J.R., and Reynolds, R.C., Jr. (1988) Application of high-gradient magnetic separation (HGMS) to structural and compositional studies of clay minerals. Journal of Sedimentary Petrology, 58, 761–763.

Thomsen, A. (1982) Preservation of porosity in the Deep Woodbine/Tuscaloosa Trend, Louisiana. Journal of Petroleum Technology, 34, 1156–1162.

Velde, B. (1989) Phyllosilicate formation in berthierine peloids and iron oolites. In Geological Society Special Publication, 46, 3–8.

Velde, B., Raoult, J.-F., and Leikine, M. (1974) Metamorphosed berthierine pellets in mid-Cretaceous rocks from north-eastern Algeria. Journal of Sedimentary Petrology, 44, 1275–1280.

Walker, J.R. (1989) Polytypism of chlorite in very low grade metamorphic rocks. American Mineralogist, 74, 738–743.

——— (1993) Chlorite polytype geothermometry. Clays and Clay Minerals, 41, 260–267.

Walker, J.R., and Thompson, G.R. (1990) Structural variations in illite and chlorite in a diagenetic sequence from the Imperial Valley, California. Clays and Clay Minerals, 38, 315–321.

Warr, L.N., and Rice, A.H.N. (1994) Interlaboratory standardization and calibration of clay mineral crystallinity and crystallite size data. Journal of Metamorphic Geology, 12, 141–152.

Weaver, C.E., Highsmith, P.B., and Wampler, J.M., Eds. (1984) Chlorite. Developments in Petrology, 10, 99–139.

Whittle, C.K. (1986) Comparison of sedimentary chlorite compositions by X-ray diffraction and analytical TEM. Clay Minerals, 21, 937–947.

Wiygul, G.J., and Young, L.M. (1987) A subsurface study of the Lower Tuscaloosa Formation at Olive Field, Pike and Amity Counties, Mississippi. Transactions—Gulf Coast Association of Geological Societies, 37, 295–302.

Xu, H., and Veblen, D.R. (1993) Periodic and disordered interstratification and other microstructures in the chlorite-berthierine series. Abstracts with Programs, 105th Annual Meeting of the Geological Society of America, Boston, Massachusetts, 25, 146.

Manuscript received July 8, 1994
Manuscript accepted October 2, 1995